

Ferromagnetic Spin Ladder System: Stack of Chlorido-Bridged Dinuclear Copper(II) Complexes with 2-Methylisothiazol-3(2H)-one

Masaru Kato,^[a] Kazuo Hida,^[b] Takashi Fujihara,^[c] and Akira Nagasawa*^[a]

Keywords: Copper / Magnetic properties / Ligand effects / Ladder structures / Density functional calculations

A dinuclear copper(II) complex, $[\{\text{Cu}^{\text{II}}\text{Cl}(\text{O-mi})\}_2(\mu\text{-Cl})_2]$ [mi = 2-methylisothiazol-3(2H)-one], has been synthesized and its molecular structure in the solid state determined by single-crystal X-ray analysis. The crystal consists of centrosymmetric dinuclear copper(II) units in which each copper(II) ion is doubly bridged by two chloride ions and has a slightly distorted square-planar geometry with a terminal chlorido ligand and a terminal mi ligand coordinated through the oxygen atom. The dinuclear units stack one on top of another to form a one-dimensional two-leg ladder structure. The magnetic susceptibility of the powder was measured in the temperature range 3.0–302 K. It was found that there are ferromagnetic interactions along the rung (in the same direction

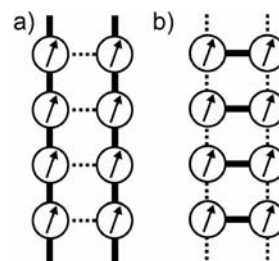
of the intramolecule; $J_{\text{rung}} = +5.03 \pm 0.03 \text{ cm}^{-1}$) and the leg (in the same direction of the intermolecule; $J_{\text{leg}} = +1.96 \pm 0.02 \text{ cm}^{-1}$) and an antiferromagnetic interaction along the diagonal ($J_{\text{x}} = -1.36 \pm 0.02 \text{ cm}^{-1}$), the experimental data being fitted by the numerical calculation for a twelve-site ladder Hamiltonian. In addition, DFT calculations with the UB3LYP functional on the model complex $[\{\text{Cu}^{\text{II}}\text{Cl}(\text{O-mi})\}_2(\mu\text{-Cl})_2]$ gave an intramolecular magnetic coupling constant $J = +28.6 \text{ cm}^{-1}$ and indicated that the spin-density distribution on O in mi is less than that on the terminal Cl. We conclude that the O-donor ligand at the terminal position plays an essential role in the emerging intramolecular ferromagnetic interaction.

Introduction

In the past decade, spin ladders have attracted much interest in the field of quantum magnetism.^[1] In particular, antiferromagnetic ladders have been investigated intensively in relation to the high- T_c superconductivity and Haldane gap problem. On the other hand, ferromagnetic ladders have been less studied, presumably because the ground state is a simple ferromagnetic state in which the quantum effect does not play a significant role. Also, from an experimental viewpoint, it is not easy to tune the bond angles to realize ferromagnetic exchange coupling in both the rung and leg directions. However, since the recent discovery of frustrated square-lattice^[2] and chain compounds^[3] with ferromagnetic nearest-neighbor coupling and antiferromagnetic next-nearest-neighbor coupling, frustrated low-dimensional ferromagnets are attracting renewed interest. The possibilities of various exotic ground states such as spin nematic and partial ferrimagnetic states have been discussed theoretically in

both one- and two-dimensional models.^[4–8] Therefore, the design and construction of ferromagnetic spin ladders are important for the experimental studies of these exotic phenomena in ladder systems. However, the construction of the ladder system in crystals is not easy compared with those of one-dimensional chains or two-dimensional network structures, because the spin ladder structure is an intermediate structure between the one-dimensional chain and the two-dimensional network. Thus, we need synthetic strategies for the efficient and easy construction of spin ladders.

Recently, two different strategies for the construction of spin ladders in the solid state were proposed by Ribas et al.,^[9] one is the combination of two one-dimensional chains, and the other is a stack of spin dimers (Scheme 1). The former method is suitable for the formation of systems in which strong $\pi\text{--}\pi$ or $\text{S}\cdots\text{S}$ interactions are expected to form two chains.^[9–11] On the other hand, the latter is appli-



Scheme 1. Two types of spin ladders: (a) Combination of two one-dimensional chains; (b) stack of spin dimers.

[a] Department of Chemistry, Graduate School of Science and Engineering, Saitama University, 255 Shimo-Okubo, Sakura-ku, Saitama 338-8570, Japan
Fax: +81-48-858-3700
E-mail: nagasawa@mail.saitama-u.ac.jp

[b] Department of Physics, Graduate School of Science and Engineering, Saitama University, Saitama 338-8570, Japan

[c] Comprehensive Analysis Center for Science, Saitama University, Saitama 338-8570, Japan

Supporting information for this article is available on the WWW under <http://dx.doi.org/10.1002/ejic.201000096>.

cable to systems such as the stack of dinuclear planar complexes^[12–14] in which the selection of ligands can tune the strength and sign of the intramolecular magnetic coupling interactions.

We have an interest in chlorido-bridged dinuclear copper(II) complexes, $[\{\text{Cu}^{\text{II}}\text{CIL}\}_2(\mu\text{-Cl})_2]^n$ (L: neutral ligand, $n = 0$; L: monoanion, $n = 2$). The magnetic properties of chlorido-bridged dinuclear copper(II) complexes have been thoroughly investigated from the viewpoint of both experiment^[15,16] and theory.^[17–20] The results suggested that the magnitude and sign of the intramolecular magnetic exchange interaction depends not only on the angle of Cu–($\mu\text{-Cl}$)–Cu but also on the type of terminal ligand L. In other words, the intramolecular magnetic interactions can be governed by the nature of the terminal ligands. In fact, antiferromagnetic and ferromagnetic interactions have been observed in the case of L = Cl^[21,22] and CH₃CN,^[23] respectively. In addition, it is known that some of these dinuclear complexes or tetrahalocuprates(II) $[\text{Cu}^{\text{II}}\text{X}_4]^{2-}$ (X = Cl, Br)^[24–26] form two-leg spin ladders in the crystal. However, it has not been confirmed yet which type of L is effective for the construction of spin ladders in crystals.

In this study we have synthesized a chlorido-bridged dinuclear copper(II) complex with 2-methylisothiazol-3(2*H*)-one (abbreviated mi, Scheme 2), $[\{\text{Cu}^{\text{II}}\text{Cl}(\text{O-mi})\}_2(\mu\text{-Cl})_2]$ (**1**) and investigated its molecular structure in the crystal. The terminal ligand mi is generally used as biocide and preservative. Thus, a number of studies relating to their biological activities have been reported, for example, investigations on mechanisms of skin sensitization,^[27] structure–activity relationships,^[28] and the effect of copper(II) ions on antimicrobial activity.^[29] However, mi is attractive as a ligand, because it is an ambidentate ligand with two opposite donor atoms according to the HSAB principle, oxygen as a hard donor atom and sulfur as a soft donor atom. Recently, it was reported that silver(I) complexes with mi form a one-dimensional chain structure in the crystal, and therefore it is expected that coordination compounds with mi form unique coordination networks.^[30]



Scheme 2. Molecular structure of 2-methylisothiazol-3(2*H*)-one.

We have also investigated the magnetic properties of **1** from an experimental and theoretical viewpoint. In this study density functional theory (DFT) calculations have been performed on model complex **1** and $[\{\text{Cu}^{\text{II}}\text{Cl}_2\}_2(\mu\text{-Cl})_2]^{2-}$. DFT calculations are a powerful tool for investigating magnetic coupling interactions. We have elucidated the influence of the terminal ligand mi on the whole spin ladder and the intramolecular magnetic interaction. We propose herein a key to the strategy for the construction of an effective spin-ladder system based on these results.

Results and Discussion

Crystal Structure

The dinuclear copper(II) complex with mi, $[\{\text{Cu}^{\text{II}}\text{Cl}(\text{O-mi})\}_2(\mu\text{-Cl})_2]$ (**1**), was synthesized and the molecular structure determined by single-crystal X-ray analysis. The molecular structure of **1** consists of a centrosymmetric dinuclear copper(II) unit as shown in Figure 1. Each copper(II) ion is in a slightly distorted square-planar geometry, and the mi molecules coordinate to the copper(II) ion through the oxygen atom as a monodentate ligand. The O(1)–Cu(1)–Cl(2) angle is 163.78(13)°, and the largest deviation of the oxygen atom from the plane is 0.3756(44) Å.

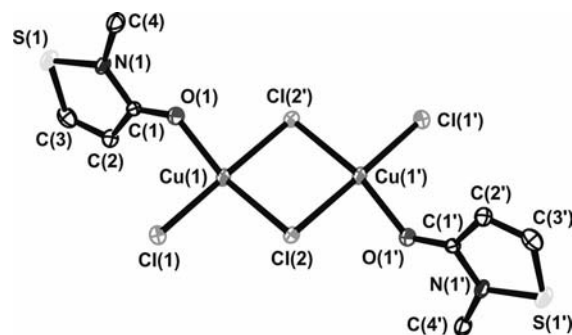


Figure 1. ORTEP drawing of **1** with atomic labeling scheme. Hydrogen atoms have been omitted for clarity.

Selected bond lengths and angles are listed in Table 1. The Cu–Cl distances are different for the bridging ($\mu\text{-Cl}$) and terminal ($\eta\text{-Cl}$) ligands: The Cu–($\mu\text{-Cl}$) distances [2.3226(15) and 2.2816(15) Å] are longer than the Cu–($\eta\text{-Cl}$) distance [2.2612(15) Å]. Furthermore, the Cu–($\mu\text{-Cl}$) bond *trans* to mi [2.2816(15) Å] is shorter than that *trans* to ($\eta\text{-Cl}$) [2.3226(15) Å]. The distance between the two copper(II) ions, 3.4055(14) Å, is larger than the sum of two ionic radii of the copper(II) ion (1.14 Å),^[31] which suggests no direct electronic interaction between the two copper(II) ions.

Table 1. Selected bond lengths and angles for **1**.

Bond	Length [Å]	Bond	Angle [°]
C(1)–O(1)	1.241(6)	Cu(1)–Cl(2)–Cu(1') ^[a]	95.40(5)
C(1)–N(1)	1.356(6)	O(1)–Cu(1)–Cl(1)	94.38(12)
C(1)–C(2)	1.430(7)	O(1)–Cu(1)–Cl(2)	163.78(13)
C(2)–C(3)	1.325(7)	Cl(1)–Cu(1)–Cl(2)	93.28(5)
C(3)–S(1)	1.707(6)	O(1)–Cu(1)–Cl(2) ^[a]	86.74(12)
C(4)–N(1)	1.463(6)	Cl(1)–Cu(1)–Cl(2) ^[a]	175.61(6)
Cl(1)–Cu(1)	2.2612(15)	Cl(2)–Cu(1)–Cl(2) ^[a]	84.60(5)
Cl(2)–Cu(1)	2.2816(15)	C(1)–N(1)–S(1)	114.7(4)
Cl(2)–Cu(1) ^[a]	2.3226(15)	C(1)–O(1)–Cu(1)	133.5(4)
Cu(1)–O(1)	1.941(4)	N(1)–S(1)–C(3)	89.9(3)
N(1)–S(1)	1.690(5)		
Cu(1)–Cu(1') ^[a]	3.4055(14)		
Cl(1)–Cu(1) ^[b]	2.8851(16)		
Cl(2)–Cu(1) ^[c]	3.0410(15)		

[a] $-x, -y, 1 - z$. [b] $1 + x, y, z$. [c] $1 - x, -y, 1 - z$.

In the crystal, the discrete dinuclear copper(II) units stack one on top of another to form a one-dimensional two-leg ladder structure. As illustrated in Figure 2, each ter-

terminal and bridging chlorido ligand in other units occupy the fifth and sixth coordination sites of the copper atom. The Cu–(η -Cl) and Cu–(μ -Cl) distances between the units are 3.0410(15) and 2.8851(16) Å, respectively. This stacking pattern is similar to those of dinuclear copper(II) complexes such as $K_2[\{Cu^{II}Cl_2\}_2(\mu-Cl)_2]$,^[32] $[\{Cu^{II}Br(py)\}_2(\mu-Br)_2]$ (py = pyridine),^[33] or $[\{Cu^{II}Cl(CH_3CN)\}_2(\mu-Cl)_2]$ ^[23] complexes, which form one-dimensional two-leg ladder structures. These results indicate that the Cu–Cl intermolecular interaction could induce the self-assembly construction of a one-dimensional spin ladder if we could obtain a Cu(μ -Cl)₂Cu unit. Furthermore, π – π interactions between mi molecules may support the construction of the ladder, because mi has a planar five-membered ring in which the largest deviation of C(1) from the ring [S(1)/N(1)/C(1)–C(3)] is 0.0072(32) Å, and the distance between mi molecules is 3.843 Å. Consequently, the Cu–Cl intermolecular and π – π interactions may play an important role in the self-assembly construction of the spin ladder in the present system.

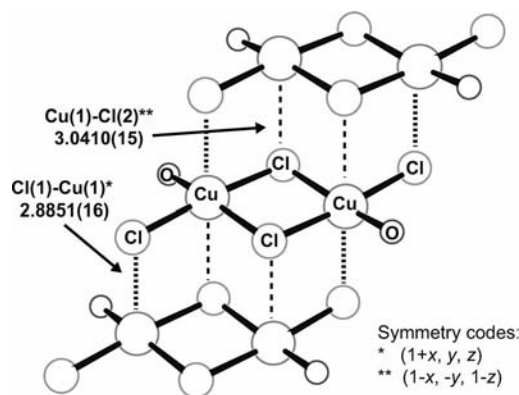


Figure 2. Stacking of $[\{Cu^{II}Cl(O-mi)\}_2(\mu-Cl)_2]$ units in the crystal with selected bond lengths.

For the construction of the ladder, the selection of the terminal ligand L is important. For several decades, many $Cu(\mu-Cl)_2Cu$ complexes with polydentate ligands L have been investigated;^[16,18,19,34] however, there is no report of their formation as spin ladders. These results suggest that polydentate ligands tend to induce the formation of discrete $Cu(\mu-Cl)_2Cu$ complexes. Furthermore, the use of bulky monodentate ligands may not be favorable for the construction of spin-ladder structures. $Cu(\mu-Cl)_2Cu$ complexes containing monodentate ligands, for example, $[\{Cu^{II}Cl(tempo)\}_2(\mu-Cl)_2]$ (tempo = 2,2,6,6-tetramethylpiperidine-1-oxyl),^[35] $[\{Cu^{II}Cl(Me_3SiNPMMe_3)\}_2(\mu-Cl)_2]$,^[36] and $[\{Cu^{II}Cl(Me_3SiNPPH_3)\}_2(\mu-Cl)_2]$,^[37] have been synthesized; however, they did not form spin-ladder structures in the crystal. In summary, the use of monodentate ligands, but not bulky ones, may be suitable for the construction of the ladder structure.

Magnetic Behavior

The temperature dependence of the susceptibility was measured in the temperature range 3.0–302 K. The plot of

$\chi_M T$ versus T for **1** is shown in Figure 3a, with χ_M being the molar magnetic susceptibility per Cu^{II} ion. At 302 K, $\chi_M T = 0.39 \text{ cm}^3 \text{ mol}^{-1} \text{ K}$, which is slightly higher than the theoretically expected value ($0.38 \text{ cm}^3 \text{ mol}^{-1} \text{ K}$) for an isolated copper(II) ion ($S = 1/2$, $g = 2$). The $\chi_M T$ value gradually increases upon cooling to around 20 K, and then it sharply increases to $0.9 \text{ cm}^3 \text{ mol}^{-1} \text{ K}$ at 3.0 K. It is clear that ferromagnetic exchange interactions exist between the copper(II) ions. The plot of χ_M^{-1} versus T in the temperature range 200–302 K is shown in the inset of Figure 3a from which a Weiss temperature θ of $+8.97 \pm 0.97 \text{ K}$ is obtained. This plot also indicates ferromagnetic behavior. Nevertheless, no anomaly suggesting a phase transition to a magnetically ordered phase is observed down to the lowest temperature. These results may be attributed to the spin-ladder

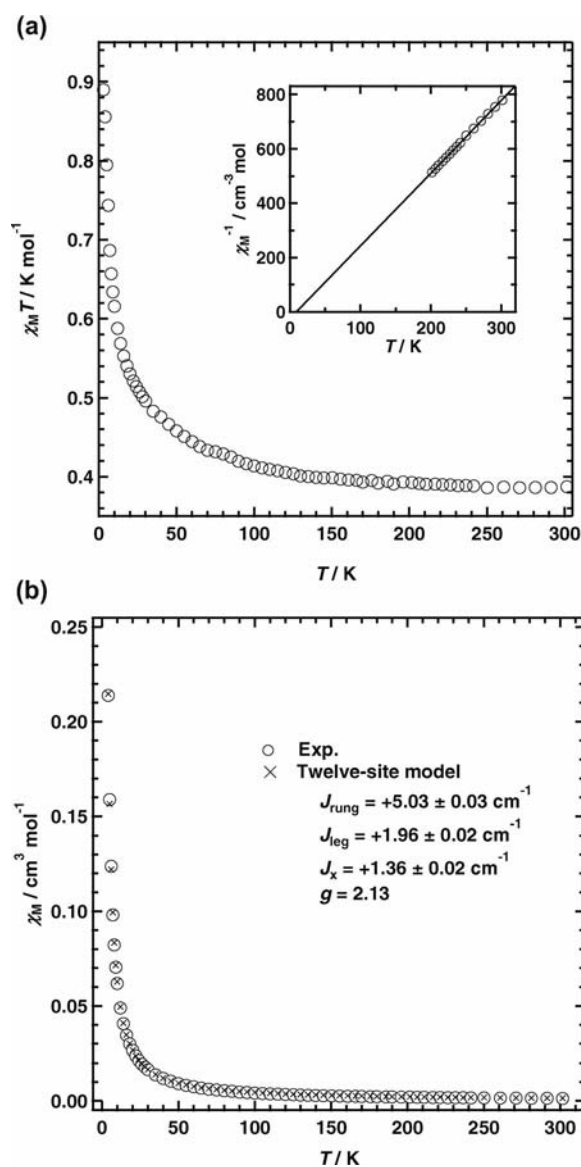


Figure 3. (a) Temperature dependence of $\chi_M T$ for **1** per Cu ion. Inset: temperature dependence of χ_M^{-1} (Currie–Weiss plot). (b) Experimental data of χ_M (○) and the data fit by using the twelve-site model function (×).

structure of **1**, that is, the low-dimensional spin alignment such as the spin ladder prevents three-dimensional ferromagnetic ordering at the lowest temperature.

Comparison with dinuclear copper(II) complexes with two bridging chlorido ligands shows that the magnetic behavior of the present system is similar to that of $[\{\text{Cu}^{\text{II}}\text{Cl}(\text{CH}_3\text{CN})\}_2(\mu\text{-Cl})_2]$, in which ferromagnetic coupling is observed,^[23] but is different to those of $(\text{DBTTF})_2[(\text{Cu}^{\text{II}}\text{Cl}_2)_2(\mu\text{-Cl})_2]$ ^[18] or $\text{K}[(\text{Cu}^{\text{II}}\text{Cl}_2)_2(\mu\text{-Cl})_2]$ ^[21] complexes, which show antiferromagnetic behavior. Selected bond lengths and angles for these complexes are summarized in Table 2. We have found that the Cu–Cl–Cu bridging angles for ferromagnetic $[\{\text{Cu}^{\text{II}}\text{Cl}\}_2(\mu\text{-Cl})_2]^n$ complexes are slightly smaller than those for antiferromagnetic complexes; however, it cannot be concluded that these bond angles depend on the magnetic properties of the $[\{\text{Cu}^{\text{II}}\text{Cl}\}_2(\mu\text{-Cl})_2]^n$ complexes. In addition, there is no relationship between the longer Cu–Cl distance in the bridge and the magnetic properties. Thus, these results indicate that the terminal ligand in $[\{\text{Cu}^{\text{II}}\text{Cl}\}_2(\mu\text{-Cl})_2]^n$ plays a significant role in determining the intramolecular magnetic coupling interactions between the copper(II) ions.

Table 2. Selected bond lengths and angles for $[\{\text{Cu}^{\text{II}}\text{Cl}\}_2(\mu\text{-Cl})_2]^n$.

L	Cl ^[a]	Cl ^[b]	O-mi	CH ₃ CN
Cu–Cl ^[c] [Å]	2.297(1)	2.322	2.3226(15)	2.31
Cu–(μ-Cl)–Cu [°]	96.24(6)	95.9	95.40(5)	94
Magnetism ^[d]	AF	AF	F	F
Ref.	[18,38]	[21,32]	this work	[23,39]

[a] $(\text{DBTTF})_2[\{\text{Cu}^{\text{II}}\text{Cl}_2\}_2(\mu\text{-Cl})_2]$. [b] $\text{K}_2[\{\text{Cu}^{\text{II}}\text{Cl}_2\}_2(\mu\text{-Cl})_2]$. [c] The longer Cu–Cl distance in the bridge. [d] AF: antiferromagnetic behavior; F: ferromagnetic behavior.

As mentioned above, a copper(II) dinuclear complex forms a one-dimensional ladder structure in the solid state with four magnetic exchange pathways illustrated in Figure 4. Therefore, we tried to fit the temperature dependence of the magnetic susceptibility by numerically diagonalizing the finite length ladder Heisenberg Hamiltonian according to Equation (1) in which \hat{S}_i^r and \hat{S}_i^l are spin operators with magnitude 1/2 on the right and left legs, respectively. For the numerical calculation, the periodic boundary condition

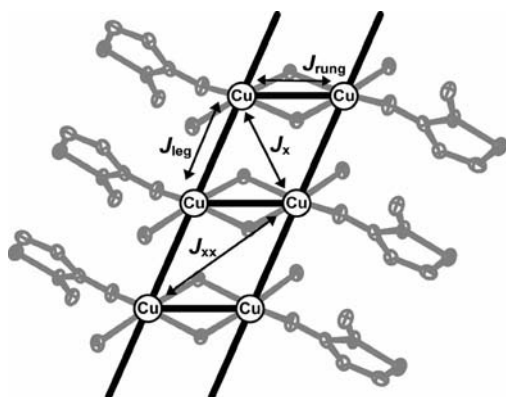


Figure 4. Representation of the two-leg ladder structure showing four different exchange pathways between two copper ions.

$\hat{S}_{N/2+1}^l = \hat{S}_1^l$ is assumed. We fitted the χ_M data using the numerical data for the twelve-site model ($N = 12$) in the temperature range 4–302 K. The best-fit parameters obtained are as follows: $J_{\text{rung}} = +5.03 \pm 0.03 \text{ cm}^{-1}$, $J_{\text{leg}} = +1.96 \pm 0.02 \text{ cm}^{-1}$, $J_x = -1.36 \pm 0.02 \text{ cm}^{-1}$, $g = 2.13$ (fixed), and $R = 1.52 \times 10^{-4}$ (in the present system the rung and leg directions are the same as the intra- and intermolecular directions, respectively; R is the agreement factor defined as $\Sigma[\chi_{M(\text{calcd.})}T - \chi_{M(\text{obsd.})}T]^2 / \Sigma[\chi_{M(\text{obsd.})}T]^2$). The fitting data reproduce the experimental results, as shown in Figure 3b. It was checked that the numerical results of χ_M for $N = 16$ are similar to those for $N = 12$ within the measured temperature range. Hence, the choice $N = 12$ is sufficient for comparison with our experimental data.

$$\hat{H}_{\text{ladder}} = \sum_{i=1}^{N/2} [-2J_{\text{leg}}(\hat{S}_i^r \cdot \hat{S}_{i+1}^r + \hat{S}_i^l \cdot \hat{S}_{i+1}^l) - 2J_{\text{rung}}\hat{S}_i^r \cdot \hat{S}_i^l - 2J_x\hat{S}_i^r \cdot \hat{S}_{i+1}^l] \quad (1)$$

Both J_{rung} and J_{leg} are positive, which means that two copper(II) ions are ferromagnetically coupled along not only the rung but also the leg. In other words, there are both intra- and intermolecular ferromagnetic interactions. This is consistent with the ferromagnetic behavior at low temperature. Interestingly, J_x is negative, which indicates the possibility of spin frustration. Strictly speaking, however, it is not conclusive that J_x actually frustrates other coupling, because the magnetic behavior is not so sensitive to J_x as long as it is small. In fact, we can also obtain a reasonable fit even if we fix $J_x = 0$ with $J_{\text{rung}} = +4.84 \pm 0.07 \text{ cm}^{-1}$, $J_{\text{leg}} = +1.034 \pm 0.006 \text{ cm}^{-1}$, $g = 2.13$ (fixed), and $R = 1.21 \times 10^{-4}$ (see the Supporting Information).

The plot of $\chi_M T^2$ versus $T^{1/2}$ for **1** in the temperature range 4–24 K is shown in Figure 5. This plot gives a quadratic function, and the least-squares fitting curve is $\chi_M T^2 = 1.0424 + 0.0661 T^{1/2} + 0.2873 T$. This behavior can be understood in terms of Takahashi's modified spin-wave theory^[40] in the following way.

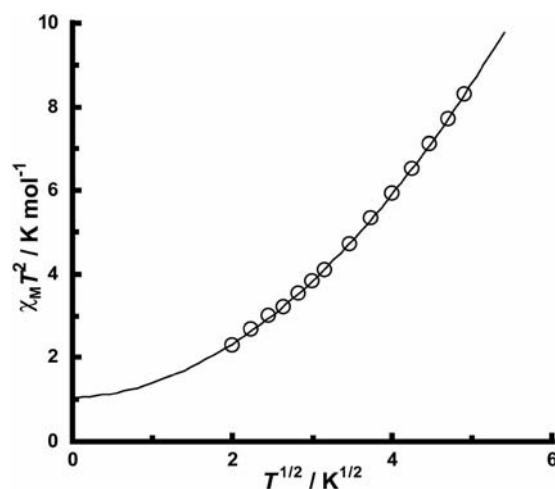


Figure 5. Plot of $\chi_M T^2$ vs. $T^{1/2}$ in the temperature range 4–24 K. The solid line represents the least-squares fitting curve $\chi_M T^2 = 1.0424 + 0.0661 T^{1/2} + 0.2873 T$.

In the present ladder compound, J_{rung} is the dominant exchange interaction. Therefore, we can approximate our model by taking the limit of strong ferromagnetic rung coupling $J_{\text{rung}} \rightarrow \infty$ and neglect the frustration terms $J_x = 0$. With this limit, the Hamiltonian given in Equation (1) reduces to the spin-1 ferromagnetic Heisenberg chain given by Equation (2) with $J = J_{\text{leg}}$ and $\hat{S}_i = \hat{S}_i^z = +\hat{S}_i^1$ is a spin-1 operator. According to ref.^[40], the relationship between magnetic susceptibility and the temperature of the spin S ferromagnetic Heisenberg chain is expressed by Equation (3) at low temperatures. Therefore, we expect that Equation (4) applies to our system substituting $S = 1$.

$$\hat{H}_{S=1} = -J_{\text{leg}} \sum_{i=1}^{N/2} \hat{S}_i \cdot \hat{S}_{i+1} \quad (2)$$

$$\frac{\chi}{(g\mu_B)^2} = \frac{2S^4 J}{3T^2} \left(1 - \frac{3}{S} \cdot (-0.582597455) \cdot \left(\frac{T}{2SJ} \right)^{1/2} + \frac{3}{S^2} \cdot (-0.582597455)^2 \cdot \left(\frac{T}{2SJ} \right) \right) \quad (3)$$

$$\frac{\chi T^2}{(g\mu_B)^2} = \frac{2J}{3} + 0.582597455 \cdot (2J)^{1/2} T^{1/2} + (-0.582597455)^2 T^{-1} \quad (4)$$

Equation (4) predicts that the intercept of the plot of $\chi_M T^2$ versus $T^{1/2}$ at $T = 0$ K is $2J/3$ K mol⁻¹ and the intercept obtained experimentally is +1.0424. Therefore, we obtain $J = J_{\text{leg}} = 1.56$ K (1.09 cm⁻¹). This value is in good agreement with that of J_{leg} (+1.034 cm⁻¹) calculated under the conditions that there is no spin frustration. These results show that ferromagnetic dinuclear copper(II) units form a ferromagnetic one-dimensional network. Although the coefficients of the second and third terms do not coincide with those obtained from the fitting, this discrepancy can be attributed to the contribution from higher-order terms and/or a finite value of J_{rung} .

The empirical correlation between J and ϕ/R was proposed for complexes with a Cu(μ -Cl)₂Cu core by Marsh et al.,^[15] with ϕ being the Cu–Cl–Cu bridging angle and R being the longer Cu–Cl distance in the bridge. From the relationship it is expected that the exchange interaction is ferromagnetic if the ϕ/R value is between 32.6 and 34.8. In the present system, values of ϕ/R are 29.8 (90.53°/3.041 Å) and 41.1° Å⁻¹ (95.41°/2.322 Å) along the rung and the leg, respectively. Therefore, our results do not follow the empirical correlation.

DFT Calculations

The magnetic measurements revealed that there is an intramolecular ferromagnetic interaction. To understand the role of the terminal ligand mi in the novel ferromagnetic interaction, we carried out DFT calculations on model complex **1** with terminal mi and a reference complex

$[\{\text{Cu}^{\text{II}}\text{Cl}_2\}_2(\mu\text{-Cl})_2]^{2-}$ (abbreviated **Cl**) with terminal Cl⁻ to estimate the difference in the intramolecular magnetic coupling constant.

The calculation gave a coupling constant of +28.6 cm⁻¹ for **1**. Although this value is slightly larger than the experimental ($J_{\text{rung}} = +5.03$ cm⁻¹), which may be attributed to a lack of consideration of intermolecular magnetic interactions, we have confirmed the observed intramolecular ferromagnetic interactions by quantum chemical calculations. For **Cl**, the calculations suggest that there is an intramolecular antiferromagnetic interaction ($J = -31.5$ cm⁻¹). This calculated coupling constant is also slightly larger than the experimental value ($J = -46.5$ cm⁻¹).^[18] In this calculation, the effects of cations or intermolecular magnetic interactions such as the Madelung effect^[24] were not taken into account. Thus, the calculated coupling constant for **Cl** may be overestimated.

Plots of spin-density distributions for the triplet states of **1** and **Cl** are illustrated in Figure 6. For all of the atoms with large spin density the spin-density values are positive, which indicates that the spin delocalization mechanism is predominant in both **1** and **Cl**.^[41] As seen in Figure 6, the spin density is mainly located on the copper(II) ions and coordinating atoms. The shape of the spin density on the copper(II) ions corresponds to the $d_{x^2-y^2}$ orbital, which is consistent with the electron configuration of the d⁹ copper ion ($t_{2g}^6 e_g^3$).

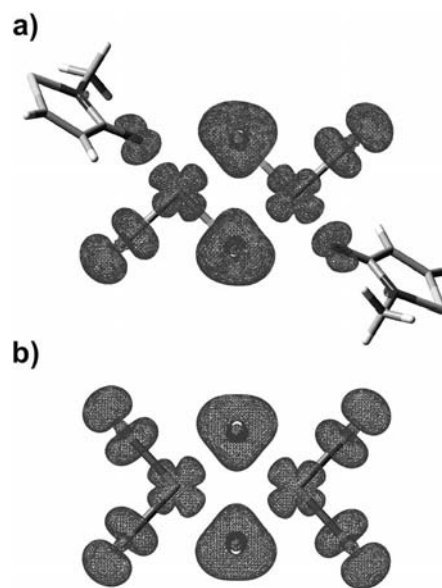


Figure 6. Spin density surfaces for (a) $[\{\text{Cu}^{\text{II}}\text{Cl}(\text{O-mi})\}_2(\mu\text{-Cl})_2]$ and (b) $[\{\text{Cu}^{\text{II}}\text{Cl}_2\}_2(\mu\text{-Cl})_2]^{2-}$ in the triplet state. The cut-off value of the isodensity surface is 0.002 e⁻ bohr⁻³.

Notably, as seen in the spin-density map for **1**, there is less spin on the oxygen atom in mi than on the terminal chlorido ligand. This difference in spin density between the O and the terminal Cl⁻ is very clearly recognized from the values of Mulliken atomic spin density listed in Table 3. Furthermore, spin densities on Cu in **1** are larger than those

in Cl. These results suggest that substitution of mi for Cl at the terminal position induces a larger spin density on the copper ion.

Table 3. Mulliken atomic spin densities and magnetic coupling constants for model complexes $[(\text{Cu}^{\text{II}}\text{ClL})_2(\mu\text{-Cl})_2]^n$ ($\text{L} = \text{O-mi}$, $n = 0$; $\text{L} = \text{Cl}$, $n = 2-$).

	O-mi	Cl
Cu	0.524	0.485
$\mu\text{-Cl}$	0.233	0.207
$\eta\text{-Cl}$	0.178	0.154
O	0.058	—
$J [\text{cm}^{-1}]$	+28.6	−31.5

As a rule of thumb, it is known that the type of atom coordinating to paramagnetic centers is important for spin-density delocalization.^[41] Previously, Cano et al. investigated the influence of the terminal ligand on the magnetic exchange coupling for model complexes $[\{\text{Cu}^{\text{II}}(\text{NH}_3)\text{X}\}_2(\mu\text{-C}_2\text{O}_4)]$ ($\text{X} = \text{F}, \text{Cl}, \text{Br}, \text{I}$) using DFT calculations.^[42] Their results indicate that the antiferromagnetic character of the exchange coupling in these complexes increases with decreasing spin density on the copper atoms. This increase in antiferromagnetic character is induced by less electronegative donors at the terminal position. These results are consistent with our results, because the coordination of the electronegative oxygen atom of mi induces an increase in spin density at the copper(II) ion.

In addition, Grigereit et al.^[17] and Rodríguez-Fortea et al.^[18] also investigated the influence of the terminal ligand on the model complexes $[(\text{Cu}^{\text{II}}\text{L}_2)_2(\mu\text{-Cl})_2]^n$ ($\text{L} = \text{N-donor ligands}$, $n = 2+$; $\text{L} = \text{Cl}$, $n = 2-$) by using the extended Hückel and DFT frameworks, respectively. Their results indicate that the antiferromagnetic coupling decreases when the terminal chlorido ligands are replaced by O- or N-donor ligands and are also consistent with our results. Therefore, we conclude that the presence of the O-donor mi at

the terminal position induces the ferromagnetic interaction for **1**.

The surface plots of the singly occupied molecular orbitals (SOMOs) of **1** are shown in Figure 7. The shape of these two SOMOs superimposed is similar to that of the spin-density distribution. In the present case, the main molecular orbitals on mi are observed at unoccupied molecular orbitals above the SOMOs, not at the SOMOs. Thus, spin-density delocalization over mi is restricted.

Conclusions

We have synthesized and characterized the dinuclear copper(II) complex $[\{\text{Cu}^{\text{II}}\text{Cl}(\text{O-mi})\}_2(\mu\text{-Cl})_2]$ with mi as terminal ligand. The dinuclear units stack one on top of another in the solid state to form a two-leg spin-ladder structure. Magnetic susceptibility measurements revealed ferromagnetic behavior coming from a one-dimensional spin ladder possibly with spin frustration. The DFT calculations suggest that the presence of the O-donor terminal ligand mi at the terminal position induces the ferromagnetic interaction within the dinuclear unit.

The results of this study suggest that the selection of an appropriate terminal ligand is important for the construction and design of the spin ladder; O-donor ligands such as isothiazol-3(2*H*)-ones or RCONHR', both with an amido moiety, are candidates for a terminal ligand L for preparing a ferromagnetically coupled system. Although no exotic phenomena due to spin frustration were observed within the measured temperature range, they could be observed at even lower temperatures and/or under high pressure. It has been pointed out that exotic ground states such as spin nematic and partial ferromagnetic states can be realized between ferromagnetic or ferrimagnetic ground states and a nonmagnetic ground state in several frustrated spin chains.^[8,43,44] It is worthwhile searching for these exotic quantum phases in this and related ladder compounds. Thus, we may conclude that the $[\{\text{Cu}^{\text{II}}\text{ClL}\}_2(\mu\text{-Cl})_2]^n$ unit is a fascinating system for the construction of spin ladders from the crystal engineering viewpoint. More systematic studies on this type of spin ladder should be carried out.

Experimental Section

Caution! Perchlorate salts are potentially explosive and should be handled with great care and in small quantities. In addition, 2-methylisothiazol-3(2*H*)-one is a skin sensitizer and should be handled with care to avoid skin contact.

Materials: 2-Methylisothiazolone hydrochloride (HmiCl) was obtained from Rohm and Haas Company. Copper(II) perchlorate hexahydrate was purchased from Kanto Chemical Co., Inc. Other reagents and solvents of reagent grade were commercially available and used without further purification.

Physical Measurements: UV/Vis spectra were recorded with Shimadzu UV-160A and JASCO V-530 spectrophotometers at room temperature. IR spectra were recorded with a Perkin-Elmer System 2000 FT-IR spectrometer at 25 °C. Elemental analyses were carried out with a FISON EA 1108 analyzer at the Molecular Analysis

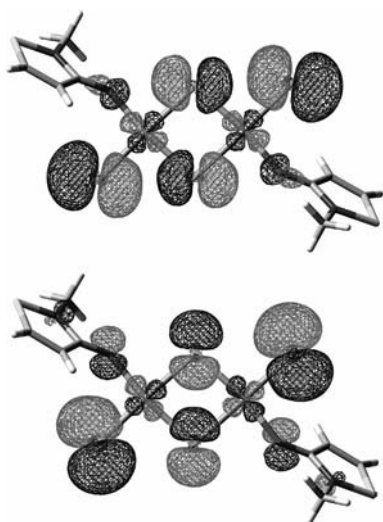


Figure 7. Surface plots of the SOMOs of $[\{\text{Cu}^{\text{II}}\text{Cl}(\text{O-mi})\}_2(\mu\text{-Cl})_2]$ in the triplet state (isovalue = $0.025 \text{ e}^- \text{ bohr}^{-3}$).

and Life Science Center, Saitama University. EPR spectra were recorded with a Bruker EMX 6/1 spectrometer at 120 K. The sample was diluted with MgSO_4 to 5% weight concentration. A g value of 2.131 was obtained (Figure S2 of the Supporting Information). Magnetic susceptibility measurements were performed with a Quantum Design MPMS-XL SQUID magnetometer in the temperature range 3.0–302 K under 10 kOe at the National Institute for Materials Science, Japan. By using Pascal's constant,^[45] the diamagnetic susceptibility was estimated to be $-219.16 \times 10^{-6} \text{ cm}^3 \text{ mol}^{-1}$ for a dinuclear complex, and the contribution was subtracted from the experimental data.

[{Cu^{II}Cl(O-mi)}₂(μ-Cl)₂] (1): HmiCl (0.044 g, 0.29 mmol) was added to a solution of $\text{Cu}(\text{ClO}_4)_2 \cdot 6\text{H}_2\text{O}$ (0.033 g, 0.089 mmol) in EtOH (5 cm³). The resulting light yellow solution was stirred at room temperature overnight, and the solvent was then removed at ambient temperature under vacuum. The crude product was recrystallized from a solution in acetone/ethyl acetate at room temperature. An orange precipitate was isolated by suction filtration and dried under vacuum. Yield: 0.035 g (79% based on the Cu salt). $\text{C}_8\text{H}_{10}\text{Cl}_4\text{Cu}_2\text{N}_2\text{O}_2\text{S}_2$ (499.21): calcd. C 19.25, H 2.02, N 5.61; found C 19.11, H 1.88, N 5.66. UV/Vis (acetone): λ_{max} (ϵ) = 471 (520×10^3), 840 (br., $140 \times 10^3 \text{ cm}^2 \text{ mol}^{-1}$) nm. IR (KBr): $\tilde{\nu}$ = 1596 (C=O) cm⁻¹.

X-ray Structural Determination: Single crystals of **1** suitable for X-ray diffraction analysis were grown by slow concentration of a solution in acetone at 273 K. Measurements were carried out with a Bruker SMART APEX CCD system equipped with a graphite-monochromated Mo- K_α X-ray source (λ = 0.71073 Å) at 173 K. Absorption correction was applied by using the program SADABS.^[46] The structure was solved by direct methods using the SHELXTL-NT software.^[47] Non-hydrogen atoms were refined anisotropically. Hydrogen atoms were included and refined by using a riding model. Crystallographic data and structure refinement for **1** are shown in Table 4.

Table 4. Crystallographic data and structure refinement for **1**.

Empirical formula	C ₈ H ₁₀ Cl ₄ Cu ₂ NOS
Formula mass	249.61
Crystal system	monoclinic
Space group	$P2_1/n$
a [Å]	3.8434(8)
b [Å]	15.597(4)
c [Å]	12.810(3)
α [°]	90
β [°]	96.930(7)
γ [°]	90
V [Å ³]	762.3(3)
Z	4
T [K]	173(2)
Crystal size [mm]	$0.22 \times 0.08 \times 0.06$
μ [mm ⁻¹]	3.762
$D_{\text{calcd.}}$ [Mg m ⁻³]	2.175
Collected data	5520
Parameters	92
R_1, wR_2 [$I > 2\sigma(I)$]	0.0547, 0.1010
R_1, wR_2 (all data)	0.0949, 0.1162
Max/min $\Delta\rho$ [e Å ⁻³]	0.905/−0.813

Computational Details: For a dinuclear compound containing two identical paramagnetic centers with $S_1 = S_2 = 1/2$, the Heisenberg Hamiltonian is given by Equation (5) in which J is the coupling constant and S_1 and S_2 are the local spins on centers 1 and 2, respectively. For the case of $S_1 = S_2$, the coupling constant is expressed by Equation (6) in which E_{HS} and E_{LS} are the energies of

the states with the highest and lowest total spins, respectively, and S_i is the local spin on each metal atom i .

$$\hat{H} = -2J\hat{S}_1 \cdot \hat{S}_2 \quad (5)$$

$$E_{\text{HS}} - E_{\text{LS}} = -4JS_i(S_i + 1/2) \quad (6)$$

Ruiz and co-workers reported that the coupling constants obtained by DFT calculations are in excellent agreement with those experimentally obtained when the energy of the low-spin state is simply approximated by the energy of the broken symmetry solution.^[18,48] For the case of dinuclear copper(II) complexes, by introducing $S_i = 1/2$ into Equation (6), the coupling constant can be expressed by Equation (7).

$$J = 1/2(E_{\text{BS}} - E_{\text{HS}}) \quad (7)$$

The terms E_{BS} and E_{HS} correspond to the energies of the broken-symmetry singlet and triplet state, respectively. In this study, coupling constants were obtained by using Equation (7). All the DFT calculations were performed by using the Gaussian 03 program package.^[49] The UB3LYP functional^[50] was employed. The TZVP^[51] basis sets were used for all atoms. All energy calculations were performed by including the SCF = Tight option of Gaussian 03. The energy of the broken-symmetry states is obtained by using the Stable = Opt option.^[52] Magnetic exchange coupling constants were estimated from single-point calculations of the initial geometries. The molecular geometries determined by single-crystal X-ray analysis were used as the initial geometries. The structural data of the anion in $(\text{DBTTF})_2[\{\text{Cu}^{\text{II}}\text{Cl}_2\}_2(\mu\text{-Cl})_2]$ (DBTTF = dibenzotetraphthalvalene)^[38] were obtained from the Cambridge Structural Database (CIF CODE: CODTAQ10). The C_{2h} point group was used as a symmetry constraint for this model. The $[\{\text{Cu}^{\text{II}}\text{Cl}(\text{O-mi})\}_2(\mu\text{-Cl})_2]$ model complex was calculated with C_i symmetry. Cartesian coordinates are given in Tables S1 and S2 (see the Supporting Information).

Supporting Information (see footnote on the first page of this article): Cartesian coordinates for the model complexes $[\{\text{Cu}^{\text{II}}\text{Cl}_2\}_2(\mu\text{-Cl})_2]^{2-}$ and $[\{\text{Cu}^{\text{II}}\text{Cl}(\text{O-mi})\}_2(\mu\text{-Cl})_2]$, temperature dependence of $\chi_{\text{M}}T$ for **1** per Cu ion and data fit by using the twelve-site model function, EPR spectrum of **1**.

Acknowledgments

The authors thank Dr. Hiroaki Isago and Dr. Akiyuki Matsushita (the National Institute for Materials Science, Japan) for variable-temperature susceptibility measurements, Prof. Toshiyuki Takayanagi (Department of Chemistry, Saitama University) for useful comments on DFT calculations and Dr. Daisaku Yano (the Organo Corporation) for the gift of mi. This study was supported by the Japan Society for the Promotion of Science (JSPS) through a Grant-in-Aid for JSPS fellows (No. 21007915, to M. K.), for scientific research (C) (No.21540379, to K. H.) and for scientific research (No. 20510093, to T. F.); by the Ministry of Education, Science, Sports and Culture of Japan through a Grant-in-Aid for Scientific Research on Priority Areas ("Novel States of Matter Induced by Frustration"; No. 20046003; to K. H.); and by the Organo Corporation (to A. N.).

- [1] U. Schollwöck, J. Richter, D. J. J. Farnell, R. F. Bishop (Eds.), *Quantum Magnetism*, Springer, Berlin, Heidelberg, 2004.
- [2] H. Kageyama, T. Kitano, N. Oba, M. Nishi, S. Nagai, K. Hirota, L. Viciu, J. B. Wiley, J. Yasuda, Y. Baba, Y. Ajiro, K. Yoshimura, *J. Phys. Soc. Jpn.* **2005**, *74*, 1702–1705.

- [3] a) M. Hase, H. Kuroe, K. Ozawa, O. Suzuki, H. Kitazawa, G. Kido, T. Sekine, *Phys. Rev. B* **2004**, *70*, 104426-1–104426-6; b) S.-L. Drechsler, O. Volkova, A. N. Vasiliev, N. Tristan, J. Richter, M. Schmitt, H. Rosner, J. Málek, R. Klingeler, A. A. Zvyagin, B. Büchner, *Phys. Rev. Lett.* **2007**, *98*, 077202-1–077202-4; c) M. Enderle, C. Mukherjee, B. Fåk, R. K. Kremer, J.-M. Broto, H. Rosner, S.-L. Drechsler, J. Richter, J. Malek, A. Prokofiev, W. Assmus, S. Pujol, J.-L. Raggazzoni, H. Rakoto, M. Rheinstädter, H. M. Rønnow, *Europhys. Lett.* **2005**, *70*, 237–243.
- [4] N. Shannon, T. Momoi, P. Sindzingre, *Phys. Rev. Lett.* **2006**, *96*, 027213-1–027213-4.
- [5] A. V. Chubukov, *Phys. Rev. B* **1991**, *44*, 4693–4696.
- [6] T. Vekua, A. Honecker, H.-J. Mikeska, F. Heidrich-Meisner, *Phys. Rev. B* **2007**, *76*, 174420-1–174420-6.
- [7] L. Kecke, T. Momoi, A. Furusaki, *Phys. Rev. B* **2007**, *76*, 060407-1–060407-4.
- [8] K. Hida, *J. Phys. Soc. Jpn.* **2008**, *77*, 044707-1–044707-7.
- [9] X. Ribas, M. Tas-Torrent, A. Pérez-Benítez, J. C. Dias, H. Alves, E. B. Lopes, R. T. Henriques, E. Molins, I. C. Santos, K. Wurst, P. Foury-Leykian, M. Almeida, J. Veciana, C. Rovira, *Adv. Funct. Mater.* **2005**, *15*, 1023–1035.
- [10] J. L. Musfeldt, S. Brown, S. Mazumdar, R. T. Clay, M. Mas-Torrent, C. Rovira, J. C. Dias, R. T. Henriques, M. Almeida, *Solid State Sci.* **2008**, *10*, 1740–1744.
- [11] H. Imai, T. Otsuka, T. Naito, K. Awaga, T. Inabe, *J. Am. Chem. Soc.* **1999**, *121*, 8098–8103.
- [12] S. Sain, T. K. Maji, D. Das, J. Cheng, T.-H. Lu, J. Ribas, M. S. El Fallah, N. R. Chaudhuri, *J. Chem. Soc., Dalton Trans.* **2002**, 1302–1306.
- [13] L. Li, D. Liao, Z. Jiang, S. Yan, *Inorg. Chem.* **2002**, *41*, 1019–1021.
- [14] J. D. Woodward, R. V. Backov, K. A. Abboud, D. Dai, H.-J. Koo, M.-H. Whangbo, M. W. Meisel, D. R. Talham, *Inorg. Chem.* **2005**, *44*, 638–648.
- [15] W. E. Marsh, K. C. Patel, W. E. Hatfield, D. J. Hodgson, *Inorg. Chem.* **1983**, *22*, 511–515.
- [16] S.-L. Ma, X.-X. Sun, S. Gao, C.-M. Qi, H.-B. Huang, W.-X. Zhu, *Eur. J. Inorg. Chem.* **2007**, 846–851.
- [17] T. E. Grigereit, J. E. Drumheller, B. Scott, G. Pon, R. D. Willett, *J. Magn. Magn. Mater.* **1992**, *104*–107, 1981–1982.
- [18] A. Rodríguez-Forte, P. Alemany, S. Alvarez, E. Ruiz, *Inorg. Chem.* **2002**, *41*, 3769–3778.
- [19] M. Rodríguez, A. Llobet, M. Corbella, *Polyhedron* **2000**, *19*, 2483–2491.
- [20] P. Kapoor, A. Pathak, R. Kapoor, P. Venugopalan, M. Corbella, M. Rodríguez, J. Robles, A. Llobet, *Inorg. Chem.* **2002**, *41*, 6153–6160.
- [21] K. Hara, M. Inoue, S. Emori, M. Kubo, *J. Magn. Reson.* **1971**, *4*, 337–348.
- [22] A. Colombo, L. Menabue, A. Motori, G. C. Pellacani, W. Porzio, F. Sandrolini, R. D. Willett, *Inorg. Chem.* **1985**, *24*, 2900–2905.
- [23] C. Liu, D. R. Talham, J.-H. Park, E. Čížmár, M. W. Meisel, *J. Chem. Phys.* **2004**, *120*, 1140–1141.
- [24] M. Deumal, G. Giorgi, M. A. Robb, M. M. Turnbull, C. P. Landee, J. J. Novoa, *Eur. J. Inorg. Chem.* **2005**, 4697–4706.
- [25] A. Shapiro, C. P. Landee, M. M. Turnbull, J. Jornet, M. Deumal, J. J. Novoa, M. A. Robb, W. Lewis, *J. Am. Chem. Soc.* **2007**, *129*, 952–959.
- [26] F. Awwadi, R. D. Willett, B. Twamley, R. Schneider, C. P. Landee, *Inorg. Chem.* **2008**, *47*, 9327–9332.
- [27] a) R. Alvarez-Sánchez, D. Basketter, C. Pease, J.-P. Lepoittevin, *Chem. Res. Toxicol.* **2003**, *16*, 627–636; b) R. Alvarez-Sánchez, D. Basketter, C. Pease, J.-P. Lepoittevin, *Bioorg. Med. Chem. Lett.* **2004**, *14*, 365–368.
- [28] a) J. O. Morley, A. J. O. Kapur, M. H. Charlton, *Org. Biomol. Chem.* **2005**, *3*, 3713–3719; b) A. Khalaj, N. Adibpour, A. R. Shahverdi, M. Daneshmand, *Eur. J. Med. Chem.* **2004**, *39*, 699–705; c) K. Taubert, S. Kraus, B. Schulze, *Sulfur Rep.* **2002**, *23*, 79–121.
- [29] V. F. Riha, M. Sondossi, H. W. Rossmore, *Int. Biodeterioration* **1990**, *26*, 303–313.
- [30] M. Kato, T. Fujihara, D. Yano, A. Nagasawa, *CrystEngComm* **2008**, *10*, 1460–1466.
- [31] W. L. Jolly in *Modern Inorganic Chemistry*, 2nd ed., McGraw-Hill, New York, **1991**.
- [32] R. D. Willett, C. Dwiggen, R. F. Kruh, R. E. Rundle, *J. Chem. Phys.* **1963**, *38*, 2429–2436.
- [33] D. D. Swank, R. D. Willett, *Inorg. Chem.* **1980**, *19*, 2321–2323.
- [34] M. Rodríguez, A. Llobet, M. Corbella, A. E. Martell, J. Reibenspies, *Inorg. Chem.* **1999**, *38*, 2328–2334.
- [35] J. Laugier, J.-M. Latour, A. Caneschi, P. Rey, *Inorg. Chem.* **1991**, *30*, 4474–4477.
- [36] T. Miekisch, H. J. Mai, R. M. Z. Köcker, K. Dehnicke, J. Magull, H. Goesmann, *Z. Anorg. Allg. Chem.* **1996**, *622*, 583–588.
- [37] D. Fenske, E. Böhm, K. Dehnicke, J. Strähle, *Z. Naturforsch. Teil B* **1988**, *43*, 1–4.
- [38] M. Honda, C. Katayama, J. Tanaka, M. Tanaka, *Acta Crystallogr., Sect. C* **1985**, *41*, 197–199.
- [39] R. D. Willett, R. E. Rundle, *J. Chem. Phys.* **1964**, *40*, 838–847.
- [40] M. Takahashi, *Progress. Theor. Phys. Suppl.* **1986**, *87*, 233–246.
- [41] E. Ruiz, J. Cirera, S. Alvarez, *Coord. Chem. Rev.* **2005**, *249*, 2649–2660.
- [42] J. Cano, E. Ruiz, S. Alvarez, M. Verdager, *Comments Inorg. Chem.* **1998**, *20*, 27–56.
- [43] S. Yoshikawa, S. Miyashita, *J. Phys. Soc. Jpn.* **2005**, *74*, Suppl. 71–74.
- [44] K. Hida, *J. Phys. Condens. Matter* **2007**, *19*, 145225-1–145225-6.
- [45] G. A. Bain, J. F. Berry, *J. Chem. Educ.* **2008**, *85*, 532–536.
- [46] G. M. Sheldrick, *SADABS*, University of Göttingen, Germany, **1996**.
- [47] G. M. Sheldrick, *SHELXTL*, DOS/Windows/NT Version 6.12, Bruker AXS Inc., Madison, Wisconsin, USA, **2001**.
- [48] a) A. Rodríguez-Forte, E. Ruiz, S. Alvarez, P. Alemany, *Dalton Trans.* **2005**, 2624–2629; b) E. Ruiz, P. Alemany, S. Alvarez, J. Cano, *J. Am. Chem. Soc.* **1997**, *119*, 1297–1303; c) E. Ruiz, P. Alemany, S. Alvarez, J. Cano, *Inorg. Chem.* **1997**, *36*, 3683–3688.
- [49] M. J. Frisch, G. W. Trucks, H. B. Schlegel, G. E. Scuseria, M. A. Robb, J. R. Cheeseman, J. A. Montgomery Jr., T. Vreven, K. N. Kudin, J. C. Burant, J. M. Millam, S. S. Iyengar, J. Tomasi, V. Barone, B. Mennucci, M. Cossi, G. Scalmani, N. Rega, G. A. Petersson, H. Nakatsuji, M. Hada, M. Ehara, K. Toyota, R. Fukuda, J. Hasegawa, M. Ishida, T. Nakajima, Y. Honda, O. Kitao, H. Nakai, M. Klene, X. Li, J. E. Knox, H. P. Hratchian, J. B. Cross, C. Adamo, J. Jaramillo, R. Gomperts, R. E. Stratmann, O. Yazyev, A. J. Austin, R. Cammi, C. Pomelli, J. W. Ochterski, P. Y. Ayala, K. Morokuma, G. A. Voth, P. Salvador, J. J. Dannenberg, V. G. Zakrzewski, S. Dapprich, A. D. Daniels, M. C. Strain, O. Farkas, D. K. Malick, A. D. Rabuck, K. Raghavachari, J. B. Foresman, J. V. Ortiz, Q. Cui, A. G. Baboul, S. Clifford, J. Cioslowski, B. B. Stefanov, G. Liu, A. Liashenko, P. Piskorz, I. Komaromi, R. L. Martin, D. J. Fox, T. Keith, M. A. Al-Laham, C. Y. Peng, A. Nanayakkara, M. Challacombe, P. M. W. Gill, B. Johnson, W. Chen, M. W. Wong, C. Gonzalez, J. A. Pople, *Gaussian 03*, Revision D.02, Gaussian, Wallingford, CT, **2004**.
- [50] A. D. Becke, *J. Chem. Phys.* **1993**, *98*, 5648–5652.
- [51] A. Schaefer, C. Huber, R. Ahlrichs, *J. Chem. Phys.* **1994**, *100*, 5829–5835.
- [52] R. Bauernschmitt, R. Ahlrichs, *J. Chem. Phys.* **1996**, *104*, 9047–9052.

Received: January 29, 2010

Revised version received: October 10, 2010

Published Online: December 14, 2010